

Preparation of $\text{Al}_{2-x}\text{Y}_x\text{W}_3\text{O}_{12}$ powders by citrate sol-gel process

ZHANG Hai-jun(张海军), ZHANG Qing(张青), JIA Quan-li(贾全利), YE Guo-tian(叶国田)

High Temperature Ceramics Institute, Zhengzhou University, Zhengzhou 450052, China

Received 12 December 2007; accepted 23 April 2008

Abstract: $\text{Al}_{2-x}\text{Y}_x\text{W}_3\text{O}_{12}$ ($x=0.2, 0.5, 0.8, 1.0, 1.2, 1.5, 1.7$ and 2.0) powders were synthesized by citrate sol-gel process. The concentration of species in a citric solution for preparing $\text{Al}_{2-x}\text{Y}_x\text{W}_3\text{O}_{12}$ powders was calculated. The powders were characterized by differential thermal analysis(DTA), thermogravimetry(TG), X-ray diffractometry(XRD) and scanning electron microscopy(SEM), respectively. No solid solution of $\text{Al}_{2-x}\text{Y}_x\text{W}_3\text{O}_{12}$ is formed with x values varying from 0 to 2.0. The maximum solid solubility of Y_2O_3 in $\text{Al}_2\text{W}_3\text{O}_{12}$ and Al_2O_3 in $\text{Y}_2\text{W}_3\text{O}_{12}$ is less than 0.5. $\text{Y}_2\text{W}_3\text{O}_{12}$ easily absorbs water in air and forms a composition of $\text{Y}_2\text{W}_3\text{O}_{12} \cdot 3.2\text{H}_2\text{O}$, and $\text{Al}_2\text{W}_3\text{O}_{12}$ forms $\text{Al}_2\text{W}_3\text{O}_{12} \cdot 0.17\text{H}_2\text{O}$ in the same condition.

Key words: $\text{Al}_{2-x}\text{Y}_x\text{W}_3\text{O}_{12}$; citrate sol-gel; preparation; hydration

1 Introduction

Most substances expand during heating. Recently, materials that exhibit negative thermal expansion(NTE) have attracted considerable interest because of the potential to prepare composite materials with a specific coefficient of thermal expansion, positive, negative, or zero in some specific temperature range. There are many materials that exhibit negative thermal expansion such as zeolites, β -quartz, some AMO_3 oxides (such as BaTiO_3 , PbTiO_3) with the perovskite structure[1], compounds with general formula $\text{A}_2(\text{MO}_4)_3$ (A: trivalent cations and M: W^{6+} , Mo^{6+} , etc)[2–3], and compounds such as ZrMo_2O_8 , HfMo_2O_8 , Zn_2GeO_4 [4] and $\text{Zr}_{1-x}\text{Hf}_x\text{W}_2\text{O}_8$ [5], ZrW_2O_8 [6–7].

It is well known that the Pechini or citrate sol-gel process is usually considered to have the advantage of even mixing of starting materials, and easy control of the accurate composition of the final products[8–11]. To the knowledge of authors, there are still very few reports on the preparation of $\text{Y}_2\text{W}_3\text{O}_{12}$ and $\text{Al}_2\text{W}_3\text{O}_{12}$ powders by a homogeneous sol-gel process, as most of reported $\text{Y}_2\text{W}_3\text{O}_{12}$ and $\text{Al}_2\text{W}_3\text{O}_{12}$ powders are synthesized by classical solid-mixing-reaction method[12–16]. In this work, the citrate sol-gel process is used to prepare $\text{Al}_{2-x}\text{Y}_x\text{W}_3\text{O}_{12}$ powders. A model is used to evaluate the influence of the pH value and citric acid content on the

concentration of the cations citrate complexes in the starting solution. And the hydration of prepared $\text{Al}_2\text{W}_3\text{O}_{12}$ and $\text{Y}_2\text{W}_3\text{O}_{12}$ powders in air are also investigated.

2 Experimental

The raw materials utilized were analytical reagent grade yttrium nitrate ($\text{Y}(\text{NO}_3)_3 \cdot 6\text{H}_2\text{O}$), aluminum nitrate ($\text{Al}(\text{NO}_3)_3 \cdot 9\text{H}_2\text{O}$), ammonium tungstate ($(\text{NH}_4)_5\text{H}_5[\text{H}_2(\text{WO}_4)_6] \cdot \text{H}_2\text{O}$) and citric acid (H_3Cit). Stoichiometric amounts of yttrium nitrate and aluminum nitrate were dissolved in distilled water, and then citric acid was added. After complete mixing, ammonium tungstate and ammonia solution (about 1 mol/L) were added to get a homogenous transparent solution within a few seconds. The solution was slowly evaporated to form a highly viscous colloid, followed by heating in a temperature range of 120–140 °C for 24 h to obtain a dried gel. Finally, the dried gel precursor was calcined at 900 °C for 10 h to obtain $\text{Al}_{2-x}\text{Y}_x\text{W}_3\text{O}_{12}$ powders.

Two series of specimens were prepared for XRD tests: 1) For series A, XRD characterization was immediately carried out as soon as the sintering process was finished in order to avoid the absorption of the water; 2) For series B, XRD tests were carried out after the prepared $\text{Al}_{2-x}\text{Y}_x\text{W}_3\text{O}_{12}$ powders were held in air for about 6 months to study the moisture absorption properties

of $\text{Al}_{2-x}\text{Y}_x\text{W}_3\text{O}_{12}$ powders. The samples were characterized by PHILIPS (Model X'Pert PRO) diffractometer using $\text{Cu K}\alpha$ radiation under 40 kV and 40 mA. The XRD data were collected in the 2θ range from 10° to 70° with a step of 0.016° .

Differential thermal analysis and thermogravimetric analysis of the precursor were carried out on a NETZSCH STA-449C Thermal Analysis System with a heating rate of $10^\circ\text{C}/\text{min}$ in flowing air with sample mass of 30 mg. Platinum crucibles were used in TG-DTA analysis and the reference material was alpha-alumina. The powder morphology was observed with scanning electron microscopy (SEM) (Model JSM-5610LV, JEOL, Japan).

3 Calculation of concentration of yttrium and aluminum citrate complexes in $\text{Al}^{3+}\text{-Y}^{3+}\text{-H}_3\text{Cit}$ solution

For $\text{Al}_{2-x}\text{Y}_x\text{W}_3\text{O}_{12}$ preparation, there are several kinds of ions, such as, Y^{3+} , $\text{Y}(\text{H}_2\text{Cit})^{2+}$, $\text{Y}(\text{OH})^{2+}$, $[\text{Al}^{3+}]$, $\text{Al}(\text{Cit})$, $\text{Al}(\text{HCit})^+$, $\text{Al}(\text{OHCit})^-$, $\text{Al}(\text{OH})^{2+}$, $\text{Al}(\text{OH})_2^+$,

H_3Cit , H_2Cit^- , HCit^{2-} and Cit^{3-} existing in $\text{Al}^{3+}\text{-Y}^{3+}\text{-H}_3\text{Cit}$ solution. In order to achieve the complete homogeneity of yttrium and aluminum ions at atomic level and accurate control of the precursor composition, it is very important to increase the relative concentration of yttrium and aluminum citrate complexes, such as $\text{Y}(\text{H}_2\text{Cit})^{2+}$, $\text{Al}(\text{Cit})$ and $\text{Al}(\text{OHCit})^-$ and decreases the relative concentration of Al^{3+} and Y^{3+} . In the present work, a theoretical model similar to that in Ref.[17] was used to calculate the concentration of yttrium and aluminum citrate complexes in $\text{Al}^{3+}\text{-Y}^{3+}\text{-H}_3\text{Cit}$ solution under different conditions. The concentration of citric acid and pH value of the solution were taken into consideration.

For $\text{Al}_{1.0}\text{Y}_{1.0}\text{W}_3\text{O}_{12}$ preparation, the theoretically calculated yttrium and aluminum complex concentrations at different pH values and concentrations of citric acid are shown in Figs.1 and 2. The following phenomena can be seen from these figures.

1) The concentration of Y^{3+} and $\text{Al}(\text{Cit})$ ions decreases with pH values increasing till $\text{pH}=5$ at first, then the concentration of Y^{3+} ions increases evidently till

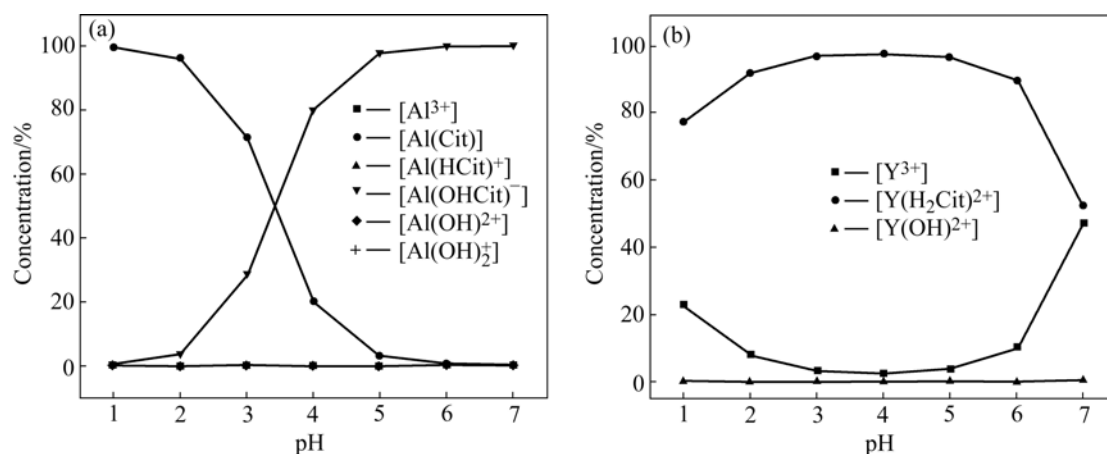


Fig.1 Evaluated concentration of aluminum and yttrium species in solution with 1:1 molar ratio of citric acid to total cations: (a) $\text{Al}^{3+}\text{-H}_3\text{Cit}$; (b) $\text{Y}^{3+}\text{-H}_3\text{Cit}$

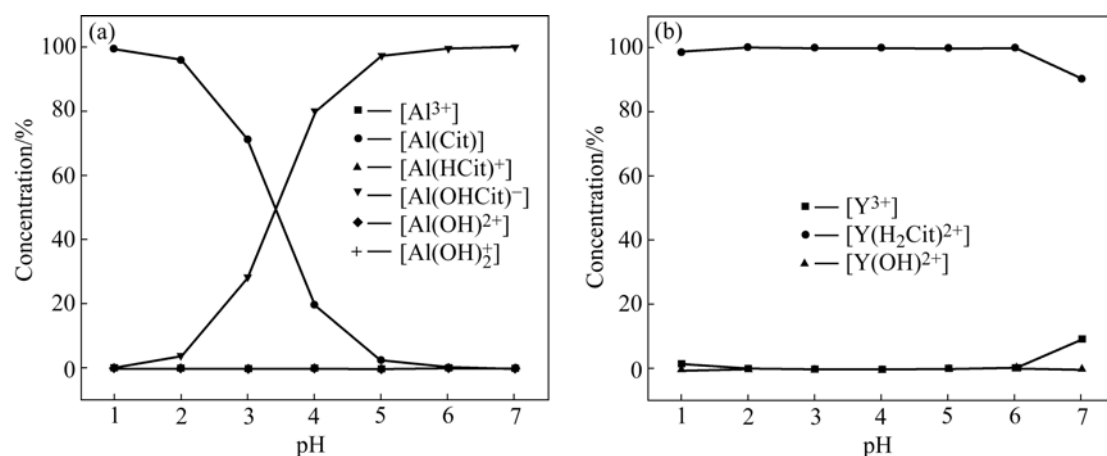


Fig.2 Evaluated concentration of aluminum and yttrium species in solution with 3:1 molar ratio of citric acid to total cations: (a) $\text{Al}^{3+}\text{-H}_3\text{Cit}$; (b) $\text{Y}^{3+}\text{-H}_3\text{Cit}$

pH=7. The concentration of $\text{Al}(\text{Cit})$ ions is about zero from pH=5 to 7. The concentration of $\text{Al}(\text{OHCit})^-$ ions increases with pH increasing. The concentration of $\text{Y}(\text{H}_2\text{Cit})^{2+}$ increases with pH increasing until pH=5, and then decreases at pH=7. The percentage of $[\text{Y}(\text{H}_2\text{Cit})^{2+}]$ to total yttrium concentration at pH=7 is only about 50% with the 1:1 molar ratio of citric acid to the total cations (Fig.1).

2) The concentration of citric acid shows a little influence on the concentration of Y^{3+} and $\text{Y}(\text{H}_2\text{Cit})^{2+}$ ions. The concentration of Y^{3+} ion decreases with increasing the citric acid content at the same pH value.

3) The concentrations of $\text{Y}(\text{OH})^{2+}$, Al^{3+} , $\text{Al}(\text{OH})^{2+}$, $\text{Al}(\text{OH})_2^+$, $\text{Al}(\text{HCit})^+$ ions are about lower than zero compared with those of $\text{Y}(\text{H}_2\text{Cit})^{2+}$, $\text{Al}(\text{Cit})$, $\text{Al}(\text{OHCit})^-$ in all conditions.

4) At pH=4 and $[\text{H}_3\text{Cit}]_{\text{T}}/\{[\text{Y}]_{\text{T}}+[\text{Al}]_{\text{T}}\}=3$, almost all yttrium and aluminum ions completely form yttrium citrate complex $\text{Y}(\text{H}_2\text{Cit})^{2+}$ and aluminum citrate complex $\text{Al}(\text{OHCit})^-$, $\text{Al}(\text{Cit})$.

According to the theoretically calculation (Figs.1 and 2), at $[\text{H}_3\text{Cit}]_{\text{T}}/\{[\text{Y}]_{\text{T}}+[\text{Al}]_{\text{T}}\}=3$ and pH=4, the percentage of the yttrium and aluminum citrate complex would increase to about 100%, indicating that $[\text{H}_3\text{Cit}]_{\text{T}}/\{[\text{Y}]_{\text{T}}+[\text{Al}]_{\text{T}}\}=3:1$ and pH=4 are suitable for $\text{Al}_{2-x}\text{Y}_x\text{W}_3\text{O}_{12}$ precursor synthesis. The calculation results are in agreement with the experimental phenomena, i.e. a transparent sol and gel with no precipitation is easily formed at the pH=4 and $[\text{H}_3\text{Cit}]_{\text{T}}/\{[\text{Y}]_{\text{T}}+[\text{Al}]_{\text{T}}\}=3:1$ in the experiment.

4 Results and discussion

4.1 TG-DTA analyses of precursor

The TG-DTA curves of the dry $\text{Al}_{1.0}\text{Y}_{1.0}\text{W}_3\text{O}_{12}$ precursor with pH=4 and $[\text{H}_3\text{Cit}]_{\text{T}}/\{[\text{Y}]_{\text{T}}+[\text{Al}]_{\text{T}}\}=3:1$ are shown in Fig.3. The mass loss can be divided into two temperature regions, namely, from room temperature to 225 °C, and from 225 °C to 751 °C. These two regions correspond to mass loss of about 40%, and 25% respectively. At higher temperature, there is almost no change in mass, which can be attributed to the formation of a pure oxide system. The exothermic peak in the first temperature region (about 225.0 °C) can be contributed to the decomposition of the citrate $\text{Y}(\text{H}_2\text{Cit})^{2+}$, $\text{Al}(\text{OHCit})^-$, $\text{Al}(\text{Cit})$, $(\text{NH}_4)_5\text{H}_5[\text{H}_2(\text{WO}_4)]_6\cdot\text{H}_2\text{O}$ and the formation of the aluminum and yttrium carbonate. The broad exothermic peaks in the second temperature region from about 400 °C to 900 °C may be caused by the decomposition of the carbonate and the formation of $\text{Al}_2\text{W}_3\text{O}_{12}$ and $\text{Y}_2\text{W}_3\text{O}_{12}$.

4.2 XRD analyses of $\text{Al}_{2-x}\text{Y}_x\text{W}_3\text{O}_{12}$ powders

The X-ray diffraction patterns of prepared

$\text{Al}_{2-x}\text{Y}_x\text{W}_3\text{O}_{12}$ calcined at 900 °C for 10 h are shown in Fig.4. It can be seen that, 1) pure $\text{Al}_2\text{W}_3\text{O}_{12}$ and $\text{Y}_2\text{W}_3\text{O}_{12}$ are prepared by citrate sol-gel methods; and 2) $\text{Al}_{2-x}\text{Y}_x\text{W}_3\text{O}_{12}$ can not form a complete solid solution as x values vary continuously from 0.0 to 2.0. The solid solubility limit of Y_2O_3 in $\text{Al}_2\text{W}_3\text{O}_{12}$ is less than 0.5 (molar fraction), and so is that of Al_2O_3 in $\text{Y}_2\text{W}_3\text{O}_{12}$.

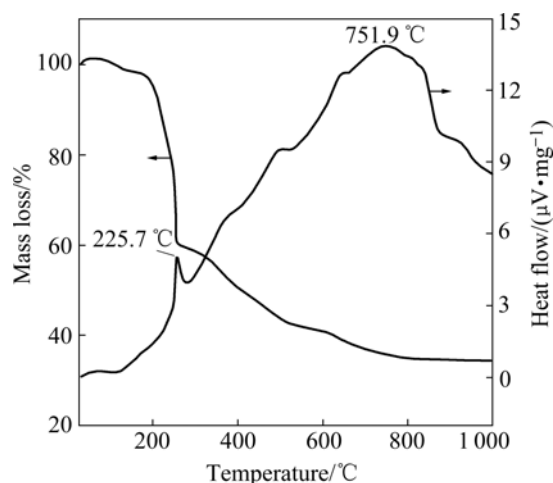


Fig.3 TG-DTA curves of $\text{Al}_{1.0}\text{Y}_{1.0}\text{W}_3\text{O}_{12}$ precursor

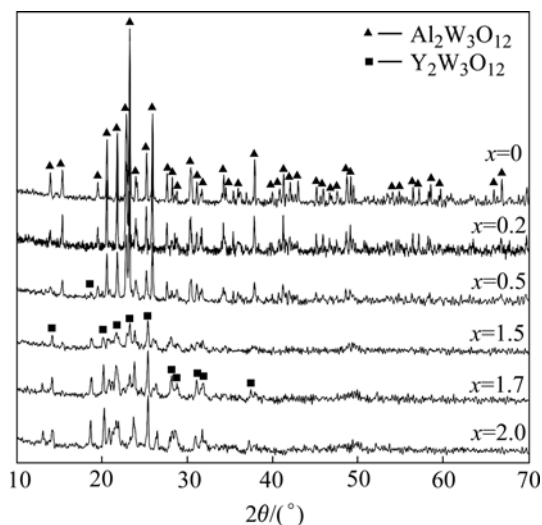


Fig.4 XRD patterns of $\text{Al}_{2-x}\text{Y}_x\text{W}_3\text{O}_{12}$ precursors annealed at 900 °C for 10 h

The XRD patterns of series A and series B of $\text{Al}_2\text{W}_3\text{O}_{12}$ and $\text{Y}_2\text{W}_3\text{O}_{12}$ specimens are shown in Fig.5. It is shown that all the diffraction peaks of series B samples (even the sample re-annealed at 800 °C) shift to high degree, indicating that the crystal cell volume of series B samples is less than that of series A samples. This result shows that water molecules can be present in the crystallographic voids and cause shrinkage of the structure. The difference in the volume of the hydrated (series B samples) and the unhydrated (series A samples) phase indicates that the water molecules cause shrinkage

of the framework structure. It is possible that the Y–O–W linkages are bent away from 180° angle in the hydrated phase. As the water is lost, the Y–O–W angle approaches the 180° linkage angle.

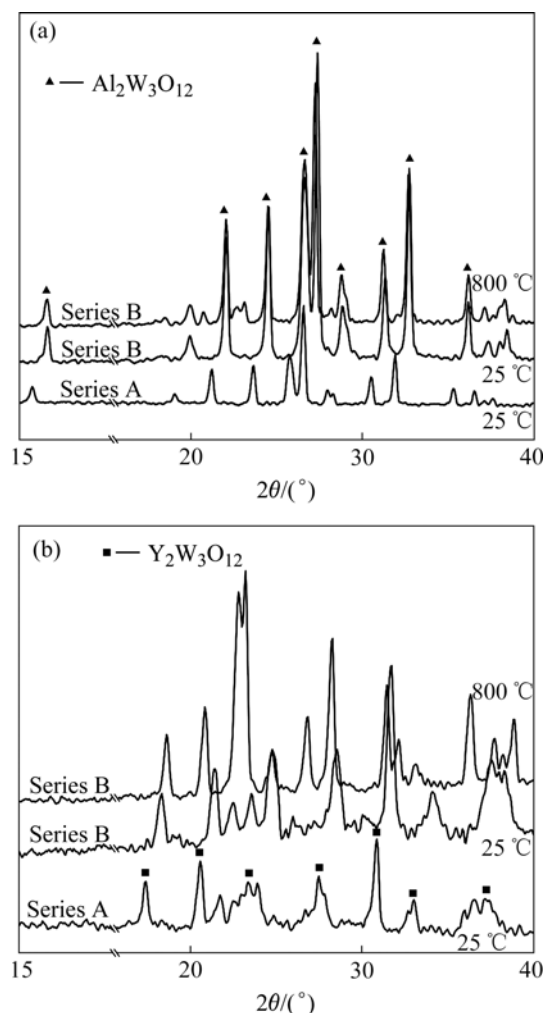


Fig.5 XRD patterns of $\text{Al}_2\text{W}_3\text{O}_{12}$ and $\text{Y}_2\text{W}_3\text{O}_{12}$ under different condition: (a) $\text{Al}_2\text{W}_3\text{O}_{12}$; (b) $\text{Y}_2\text{W}_3\text{O}_{12}$

4.3 Moisture absorbing properties of $\text{Al}_2\text{W}_3\text{O}_{12}$ and $\text{Y}_2\text{W}_3\text{O}_{12}$ powders

TG-DTA analysis of B series $\text{Al}_2\text{W}_3\text{O}_{12}$ and $\text{Y}_2\text{W}_3\text{O}_{12}$ samples is shown in Fig.6. Based on calculation, the molecule number of absorbed water in B series $\text{Y}_2\text{W}_3\text{O}_{12}$ sample hold in air for 6 months is about 3.2, which is in good agreement with the results of KARMAKAR et al[13]. The molecule number of absorbed water in B series $\text{Al}_2\text{W}_3\text{O}_{12}$ sample is about 0.17.

4.4 SEM characterization of $\text{Al}_2\text{W}_3\text{O}_{12}$ and $\text{Y}_2\text{W}_3\text{O}_{12}$ powders

The SEM micrographs of $\text{Al}_2\text{W}_3\text{O}_{12}$ and $\text{Y}_2\text{W}_3\text{O}_{12}$ samples annealed at 900 °C for 10 h are shown in Fig.7. The particles of $\text{Al}_2\text{W}_3\text{O}_{12}$ and $\text{Y}_2\text{W}_3\text{O}_{12}$ powders are

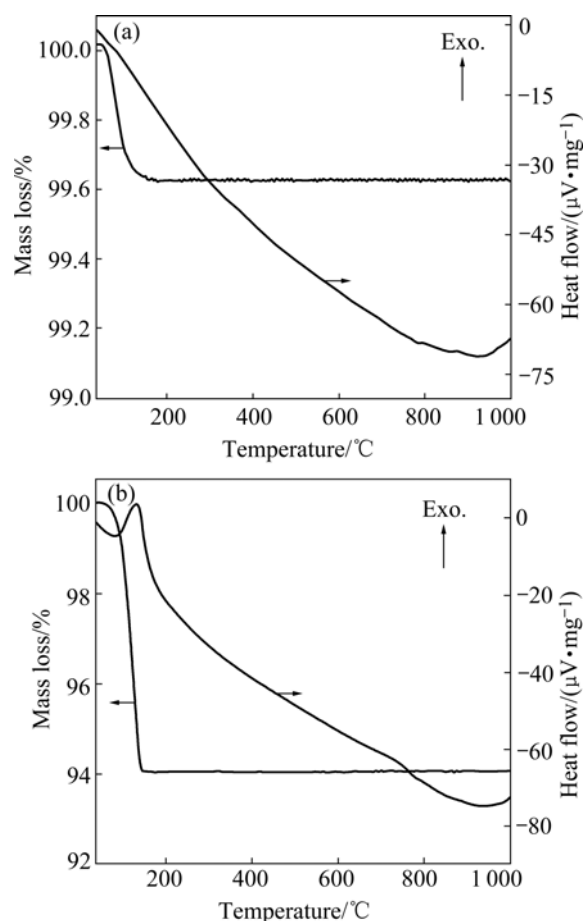


Fig.6 TG-DTA results of B series $\text{Al}_2\text{W}_3\text{O}_{12}$ (a) and $\text{Y}_2\text{W}_3\text{O}_{12}$ (b) samples

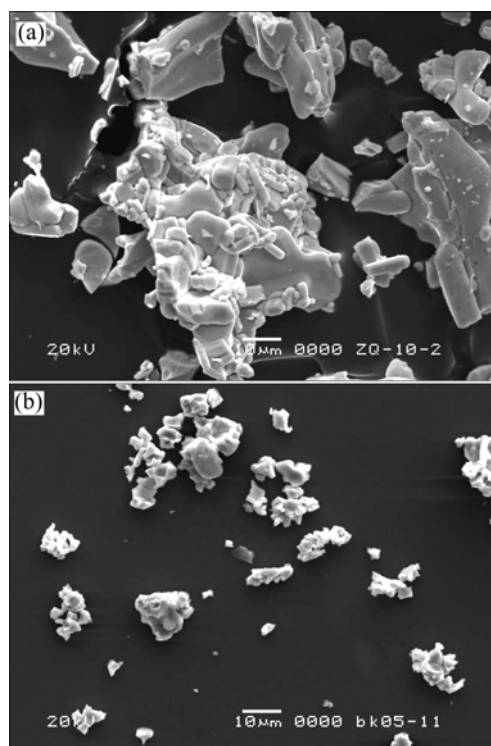


Fig.7 SEM photographs of $\text{Al}_2\text{W}_3\text{O}_{12}$ (a) and $\text{Y}_2\text{W}_3\text{O}_{12}$ (b) powder prepared at 900 °C for 10 h

widely distributed with the larger ones of more than 40 μm and the smaller ones of just 3–5 μm. It is also seen from Fig.7 that the particle size of $\text{Al}_2\text{W}_3\text{O}_{12}$ is much larger than that of $\text{Y}_2\text{W}_3\text{O}_{12}$.

5 Conclusions

1) The calculation results show that increasing the concentration of citric acid and pH values can increase the amount of yttrium and aluminum citrate, which plays a positive role in the formation of $\text{Al}_{2-x}\text{Y}_x\text{W}_3\text{O}_{12}$ gel. The concentration of those different cation citrate complexes decided by citric acid and pH values in the starting solution influences the formation of sol and further affects precipitation and segregation during gelling and charring.

2) $\text{Al}_{2-x}\text{Y}_x\text{W}_3\text{O}_{12}$ powders are formed by citrate sol-gel process using yttrium nitrate, aluminum nitrate, ammonium tungstate and citric acid as starting materials. The optimum conditions for $\text{Al}_{2-x}\text{Y}_x\text{W}_3\text{O}_{12}$ powder synthesis are $[\text{H}_3\text{Cit}]_{\text{T}}/([\text{Y}]_{\text{T}}+[\text{Al}]_{\text{T}})=3:1$, pH=4 and calcining temperature of 900 °C.

3) The maximum solid solubility of Y_2O_3 in $\text{Al}_2\text{W}_3\text{O}_{12}$ and Al_2O_3 in $\text{Y}_2\text{W}_3\text{O}_{12}$ is less than 0.5. $\text{Y}_2\text{W}_3\text{O}_{12}$ powders absorb much more water than $\text{Al}_2\text{W}_3\text{O}_{12}$ powders in air under the same condition. $\text{Y}_2\text{W}_3\text{O}_{12} \cdot 3.2\text{H}_2\text{O}$ and $\text{Al}_2\text{W}_3\text{O}_{12} \cdot 0.17\text{H}_2\text{O}$ form from $\text{Y}_2\text{W}_3\text{O}_{12}$ and $\text{Al}_2\text{W}_3\text{O}_{12}$ respectively after being left in air for 6 months.

References

- [1] SLEIGHT A W. Negative thermal expansion materials [J]. Current Opinion in Solid State & Materials Science, 1998, 3(2): 128–131.
- [2] SUMITHRA S, TYAGI A K, UMARJI A M. Negative thermal expansion in $\text{Er}_2\text{W}_3\text{O}_{12}$ and $\text{Yb}_2\text{W}_3\text{O}_{12}$ by high temperature X-ray diffraction [J]. Materials Science and Engineering B, 2005, 116(1): 14–18.
- [3] EVANS JOHN S O, MARY T A. Structural phase transitions and negative thermal expansion in $\text{Sc}_2(\text{MoO}_4)_3$ [J]. International Journal of Inorganic Materials, 2000, 2(1): 143–151.
- [4] STEVENS R, WOODFIELD B F, JULIANA B G, CRAWFORD M K. Heat capacities, third-law entropies and thermodynamic functions of the negative thermal expansion material Zn_2GeO_4 from $T=0$ to 400 K [J]. Journal of Chemical Thermodynamics, 2004, 36(5): 349–357.
- [5] NAKAJIMA N, YAMAMURA Y, TSUJI T. Phase transition of negative thermal expansion $\text{Zr}_{1-x}\text{Hf}_x\text{W}_2\text{O}_8$ solid solutions [J]. Journal of Thermal Analysis and Calorimetry, 2002, 70(2): 337–344.
- [6] TSUJI T, YAMAMURA Y, NAKAJIMA N. Thermodynamic properties of negative thermal expansion materials ZrW_2O_8 substituted for Zr site [J]. Thermochimica Acta, 2004, 416(1/2): 93–98.
- [7] STEVENS R, LINFORD J, WOODFIELD B F, JULIANA B G, LIND C, WILKINSON A P, KOWACH G. Heat capacities, third-law entropies and thermodynamic functions of the negative thermal expansion materials, cubic $\alpha\text{-ZrW}_2\text{O}_8$ and cubic ZrMo_2O_8 , from $T=(0 \text{ to } 400)$ K [J]. Journal of Chemical Thermodynamics, 2003, 35(6): 919–937.
- [8] AZADMANJIRI J. Preparation of Mn-Zn ferrite nanoparticles from chemical sol-gel combustion method and the magnetic properties after sintering [J]. Journal of Non-crystalline Solids, 2007, 353(44/46): 4170–4173.
- [9] ZHANG X Q, YUAN D R, GUO S. Sol-gel preparation of a new compound with $\text{Ca}_3\text{Ga}_2\text{Ge}_4\text{O}_{14}$ structure: $\text{La}_3\text{Al}_{5.5}\text{Ta}_{0.5}\text{O}_{14}$ [J]. Journal of Crystal Growth, 2007, 308(1): 80–83.
- [10] LAVELA P, TIRADO J L, VIDAL-ABARCA C. Sol-gel preparation of cobalt manganese mixed oxides for their use as electrode materials in lithium cells [J]. Electrochimica Acta, 2007, 52(28): 7986–7995.
- [11] KUMAR M, YADAV K L. Magnetoelectric characterization of $x\text{Ni}_{0.75}\text{Co}_{0.25}\text{Fe}_2\text{O}_4-(1-x)\text{BiFeO}_3$ nanocomposites [J]. Journal of Physics and Chemistry of Solids, 2007, 68(9): 1791–1795.
- [12] TYAGI A K, ACHARY S N, MATHEWS M D. Phase transition and negative thermal expansion in $\text{A}_2(\text{MoO}_4)_3$ system ($\text{A}=\text{Fe}^{3+}$, Cr^{3+} and Al^{3+}) [J]. Journal of Alloys and Compounds, 2002, 339(1/2): 207–210.
- [13] KARMAKAR S, DEB S K, TYAGI A K, SHARMA S M. Pressure-induced amorphization in $\text{Y}_2(\text{WO}_4)_3$: In situ X-ray diffraction and Raman studies [J]. Journal of Solid State Chemistry, 2004, 177(11): 4087–4092.
- [14] WOODCOCK D A, PHILIP L, RITTER C. Negative thermal expansion in $\text{Y}_2(\text{WO}_4)_3$ [J]. Journal of Solid State Chemistry, 2000, 149(1): 92–98.
- [15] FORSTER P M, SLEIGHT A W. Negative thermal expansion in $\text{Y}_2\text{W}_3\text{O}_{12}$ [J]. International Journal of Inorganic Materials, 1999, 1(2): 123–127.
- [16] SUMITHRA S, UMARJI A M. Hygroscopicity and bulk thermal expansion in $\text{Y}_2\text{W}_3\text{O}_{12}$ [J]. Materials Research Bulletin, 2005, 40(1): 167–176.
- [17] LEE W J, FANG T T. The effect of the molar ratio of cations and citric-acid on the synthesis of barium ferrite using a citrate process [J]. Journal of Materials Science, 1995, 30(17): 4349–435.

(Edited by YANG Bing)